New Spontaneous Fission Mode for ^{252}Cf: Indication of Hyperdeformed ^{144,145,146}Ba at Scission

G. M. Ter-Akopian,[1,2] J. H. Hamilton,[2] Yu. Ts. Oganessian,[1] A. V. Daniel,[1,2] J. Kormicki,[2,*] A. V. Ramayya,[2] G. S. Popeko,[1] B. R. S. Babu,[2] Q.-H. Lu,[2] K. Butler-Moore,[2,†] W.-C. Ma,[3] S. Ćwiok,[4,5] W. Nazarewicz,[6,7,8] J. K. Deng,[2,‡] D. Shi,[2] J. Kliman,[9] M. Morhac,[9] J. D. Cole,[10] R. Aryaeinejad,[10] N. R. Johnson,[7] I. Y. Lee,[7,§] F. K. McGowan,[7] and J. X. Saladin[5]

[1]*Joint Institute for Nuclear Research, Dubna, 141980, Russia*
[2]*Physics Department, Vanderbilt University, Nashville, Tennessee 37235*
[3]*Department of Physics, Mississippi State University, Mississippi State, Mississippi 39762*
[4]*Institute of Physics, Warsaw University of Technology, PL-00662 Warsaw, Poland*
[5]*Physics Department, University of Pittsburgh, Pittsburgh, Pennsylvania 15260*
[6]*Physics Department, University of Tennessee, Knoxville, Tennessee 37996*
[7]*Physics Division, Oak Ridge National Laboratory, Oak Ridge, Tennessee 37831*
[8]*Institute of Theoretical Physics, Warsaw University, ul. Hoża 69, PL-00681, Warsaw, Poland*
[9]*Institute of Physics, Slovak Academy of Sciences, Bratislava, Slovakia*
[10]*Idaho National Engineering Laboratory, Idaho Falls, Idaho 83415*

(Received 2 May 1995; revised manuscript received 4 March 1996)

From γ-ray coincidence studies following spontaneous fission of ^{252}Cf, direct measurements of yields and neutron multiplicities were made for Sr-Nd, Zr-Ce, Mo-Ba, Ru-Xe, and Pd-Te correlated pairs. A strong enhancement of the 7-10 neutron channels for Mo-Ba pairs is observed. A new fission mode associated with the enhanced neutron yields is identified. These data can be interpreted in terms of one or more of ^{144,145,146}Ba being hyperdeformed at scission. Mean field calculations predict a hyperdeformed third minimum in ^{252}Cf and an extremely deformed ^{146}Ba fragment at scission. [S0031-9007(96)00408-5]

PACS numbers: 25.85.Ca, 21.10.Gv, 27.60.+j, 27.90.+b

Recently we reported the first direct measurements [1] of yields and neutron multiplicities connected with the yields of correlated fragment pairs of Zr-^{146,148}Ce and Mo/Ba even-even nuclei and ^{143}Ba in the spontaneous fission (SF) of ^{252}Cf. It was noted [1] that for Mo-Ba the 0 and 8-10 neutron multiplicities were considerably higher than the gross (total) neutron multiplicities for all pairs [2]. The enhancement at high neutron multiplicity could be an indication of a new fission mode not seen previously. Indeed, two or more fission modes for the same nucleus are now known for a number of heavy nuclei undergoing SF and thermal neutron induced fission [3–8].

Here new yields for Nd/Sr, Xe/Ru, and Te/Pd correlated pairs and improved and more complete yields for the Mo/Ba and Zr/Ce pairs are presented. A comparison of our new yields for the five pairs establishes the uniqueness of the high neutron multiplicity for Mo/Ba pairs. An analysis of our new Mo-Ba data indicates a new fission mode in which the two fragments have much lower average total kinetic energy ($\overline{\mathrm{TKE}}$) than in the normal mode. The new mode includes the same Mo/Ba masses as the normal mode but the $^{144-146}$Ba fragments are hyperdeformed at scission in contrast to earlier known bimodal fission [3–8]. A brief report of this work is found in a recent review [9] with full details of the analysis to be published later separately.

The experimental details for the ORNL experiment were described earlier [1]. A similar study with ^{252}Cf was made by using Gammasphere with 36 detectors at LBNL [10]. The γ-γ matrix is a two-dimensional surface that consists mainly of three components: (1) smooth background (not full absorption of both γ), (2) two series of ridges parallel to the axes $E_{\gamma 1}$ and $E_{\gamma 2}$ (not full absorption of one γ), and (3) real peaks originating from coincidences of pairs of full absorption peaks. Because of the complexity of the spectra, a new approach to the data analysis compared to Ref. [1] was developed where the γ-γ matrix is divided into small 30×30 channel subregions. Each subregion is fitted separately with a complex two-dimensional function which includes the above components. The peaks found in component 3 make the final result of fitting procedure. For each subregion the procedure is repeated four times by shifting the boundaries in order to treat correctly peaks located near the initial subregion's boundaries.

The new yields are shown in Fig. 1 where a single Gaussian curve is fitted to each data set. A comparison of the five sets clearly shows the enhancement of the 7-10n yields for Mo/Ba. The new and more complete yields for Mo/Ba (including better efficiency corrections than in Refs. [1,10]) normalized to the known independent yields of ^{140,142,144,146}Ba [11] are presented in Table I. The new Gammasphere data [10] with lower error limits and new 10n channel confirm and extend the higher neutron multiplicity yields presented in Table I. Figure 2 shows two regions selected to enhance the weaker γ rays of interest in double gated γ spectra

 0031-9007/96/77(1)/32(4)$10.00

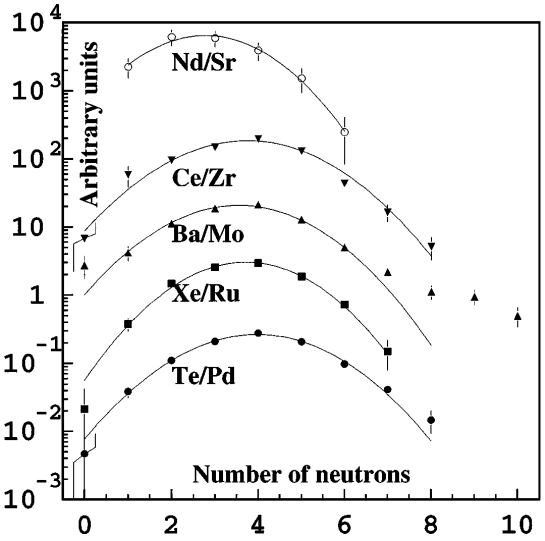

FIG. 1. Multiplicity distributions of prompt neutrons emitted at different charge splits of ^{252}Cf with Gaussian fits.

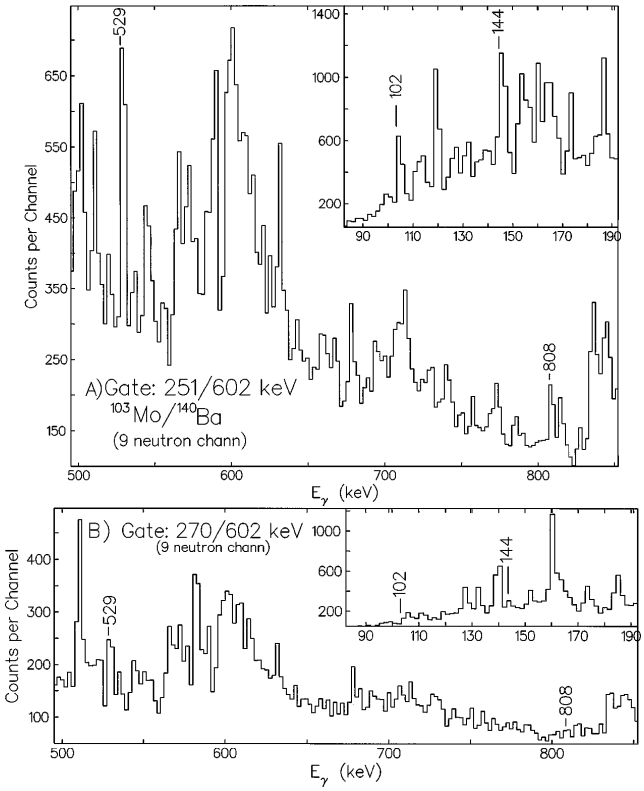

FIG. 2. Double gated spectra on (a) ^{103}Mo/^{140}Ba, and (b) background/^{140}Ba. Unlabeled lines were identified as belonging to other correlated pairs.

2(a) gating on the 251.3((7/2$^-$)-(5/2$^+$))-602.0(2$^+$-0$^+$) keV transitions in ^{103}Mo-^{140}Ba (the 9*n* channel) and 2(b) on a background to one side of the 251.3 keV peak [10]. In Fig. 2(a) one sees the 144 and 102.7 keV transitions in a (11/2$^-$)144 → (7/2$^-$)251.3 → (5/2$^+$)102.7 keV → (3/2$^+$)g.s. cascade in ^{103}Mo and all the three upper transitions in the 8$^+$(808) → 6$^+$(529) → 4$^+$(528) → 2$^+$(602 keV) → 0$^+$g.s. cascade in ^{140}Ba. If one moves either gate up or down to gate the side, on the background, all these cascade peaks either disappear or are greatly reduced as illustrated in Fig. 2(b) [10]. These results conclusively show the presence of this 9*n* channel as an example. Similar results were obtained with less statistics for the 10*n* and better statistics for the 8*n* channels.

The yields in Table I of correlated fragment pairs (Mo-Ba) and neutron multiplicities Fig. 1 originate as a result of the deexcitation of primary fission fragments. They carry information about the mass and excitation energy distributions of the primary fission fragments of fixed charge splits $Y(A_L, E_L^*, A_H, E_H^* | Z_L, Z_H)$. Here, A, Z, and E^* are the mass and atomic numbers and excitation energies of the nuclei, and subscripts L and H denote the light and heavy fragments. Yields of the fission fragment pairs $Y_i(A_L', A_H')$, created after the neutron evaporation, are directly related to the yields of the primary fission fragment pairs $Y_j(A_L, A_H)$, through the excitation energy distribution of each primary fission fragment $F(E^*, A)$, and with the probability $P_n(E^*, A)$ of evaporation of $n = A_j - A_i'$ neutrons from the primary fragment. The Mo-Ba data were unfolded to extract the distribution of primary fragments.

The unfolding was done by a least squares method. The values $Y(A_L', A_H')$ were calculated from

$$Y_i(A_L', A_H') = \sum_j Y_j(A_L, A_H) I_L I_H, \quad (1)$$

$$I_f = \int F(E_f^*, A_f) P_n(E_f^*, A_f) \delta(A_f - A_f' - n) dE, \quad (2)$$

with f being L or H.

TABLE I. Yields of correlated fragment pairs of Mo and Ba observed in the spontaneous fission of ^{252}Cf. (Yields are given in percents, i.e., in the number of pairs per 100 fission events.)

	^{138}Ba	^{140}Ba	^{142}Ba	^{143}Ba	^{144}Ba	^{145}Ba	^{146}Ba	^{147}Ba	^{148}Ba
^{102}Mo				0.02(2)	0.04(3)	0.09(6)	0.13(5)	0.10(8)	0.06(4)
^{103}Mo		0.05(3)	0.02(2)	0.13(10)	0.67(11)	0.86(24)	0.46(11)	0.40(31)	0.12(10)
^{104}Mo	0.08(3)	0.18(5)	0.36(5)	0.48(12)	1.14(17)	0.74(18)	0.39(5)	0.23(17)	0.04.(3)
^{105}Mo	0.02(2)	0.07(5)	0.65(11)	1.05(29)	1.30(22)	0.59(19)	0.13(7)	0.23(17)	
^{106}Mo	0.01(1)	0.12(3)	0.92(14)	0.88(15)	0.65(5)	0.16(8)	0.10(6)		
^{107}Mo	0.02(2)	0.12(5)	0.35(17)	0.14(8)	0.13(8)	0.14(10)			
^{108}Mo	0.02(1)	0.06(3)	0.14(5)	0.12(10)	0.06(5)				

The best fit of the calculated yields $Y_i^{\rm calc}(A_L', A_H')$ to the yields $Y_i(A_L', A_H')$ in Table I was searched by assuming Gaussian forms for the mass, excitation energy, and the distributions of primary fission fragments. The parameters $\overline{\rm TKE}$, $\sigma_{\rm TKE}$, $\overline{A}_{Hj}$, $\sigma_{A_{Hj}}$, and $\overline{E}_H^*$ were varied in the unfolding procedure. The mean excitation energies $\overline{E}_{Hj}$ were searched for nine heavy primary fragments centered around the mean mass fragment. Deexcitations of the primary fission fragments were calculated by employing the statistical code GNASH [12].

A good fit to the data of Fig. 1 is obtained only when one assumes that *two distinct fission modes* contribute to the formation of the primary Mo-Ba fission fragments, where the Mo-Ba mass and excitation energy distributions are superpositions of two Gaussians. Good fits to the data of Table I were obtained (Fig. 3) by searching for the optimal set of parameters $\overline{\rm TKE}$, $\sigma_{\rm TKE}$, $\overline{A}_H, \sigma_{A_H}$, and $\overline{E}_{Hj}^*$ for the fission Mode 1, when only one Mo-Ba primary fragment pair contributes to Mode 2. Very reasonable fits were found when the single primary fragment pair responsible for the Mode 2 is either ^{108}Mo-^{144}Ba, ^{107}Mo-^{145}Ba, or ^{106}Mo-^{146}Ba. With 16 varied parameters and 32 free points, χ^2 values of 0.92, 0.89, and 0.85, respectively, were obtained for the pairs. Each of these primary fragment pairs have essentially the same $\overline{\rm TKE} = 153 \pm 3$ MeV in Mode 2. The parameters of Mode 1 are independent of the choice of the pair contributing to Mode 2.

The characteristics extracted for the two fission modes are: Mode 1, $\overline{\rm TKE} = 189 \pm 1$ MeV, $\overline{A}_H = 145.7(1)$ and $\overline{A}_L = 106.3(1)$, $\overline{E}_{\rm Ba}^* \simeq 15$ MeV and $\overline{E}_{\rm Mo}^* \simeq 12$ MeV. Mode 2, $\overline{\rm TKE} = 153 \pm 3$ MeV and $\overline{E}_{\rm Ba}^*/\overline{E}_{\rm Mo}^* = 45.0/16.9$; 39.7/23.8; 35.4/33.2 MeV for 146/106, 145/107, 144/108, respectively. The Mode 1/Mode 2 intensity ratio for Mo/Ba is 14. The ^{106}Mo-^{146}Ba pair gives the best fit to the 7–10 neutron multiplicities as seen in Fig. 3. The data do not unambiguously determine which of the three fragment pairs or their combinations give rise to Mode 2, however, the manifestation of two distinct fission modes in the Mo-Ba split of ^{252}Cf is established unambiguously. Mode 1 looks like a familiar fission mode of ^{252}Cf in the sense that its principal characteristics $\overline{\rm TKE}$, $\sigma_{\rm TKE}$, $\overline{A}_H$, $\overline{A}_L$, and pattern of the excitation energies of the primary fragments are reasonable from what was known before [13]. What is surprising and new about Mode 2 is that the Ba fragments are left in an unusually highly excited state from which 5–8 neutrons are evaporated, and the fragments have unusually low $\overline{\rm TKE}$ which imply unusually low Coulomb energy at scission which, in turn, means enormously large elongation of the ^{252}Cf nuclei at its scission. Both features are consistent with very large deformations in the Ba fragment or fragments.

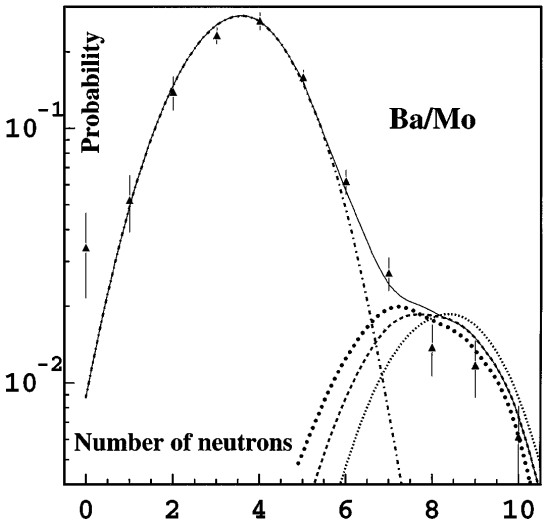

FIG. 3. The fits for Mode 2 are for 146/106 (left), 145/107 (center), and 144/108 (right).

From their large excitation energies, the barium fragments are those that are highly deformed in Mode 2. From the high excitation energies, we estimate the ratios of the axes at scission: $a/b \sim 2.8$, 3.0, and 3.2, for ^{144}Ba, ^{145}Ba, and ^{146}Ba, respectively. Thus one or more of them are hyperdeformed (HD) at scission. When the ^{106}Mo-^{146}Ba emerges in Mode 2, ^{106}Mo has about the same excitation and "normal" deformation as in Mode 1.

Potential energy surfaces of the even-even Rn, Ra, Th, and U nuclei calculated [14] by using the shell-correction approach with the axially deformed average Woods Saxon potential and the finite-range liquid drop macroscopic mass formula revealed third minima in the PES, large elongations, $\beta_2 \sim 0.9$, and significant reflection asymmetry, $0.35 \leq \beta_3 \leq 0.65$, in addition to those of the ground states ($\beta_2 \sim 0.25$) and fission isomers ($\beta_2 \sim 0.6$). Cwiok *et al.* [14] suggested that the mass distribution of fission fragments should be greatly influenced by the structure of the HD minimum and the third saddle point.

Calculations were made for ^{252}Cf similar to Ref. [14] where only a reduction of the range of Yukawa function was used to calculate the surface energy $a_{\rm surf} = 0.56$ fm. The calculated PES for ^{252}Cf for large β_2 is shown in Fig. 4(a). Three static paths to scission are shown: the symmetric path ($\beta_3 = 0$) associated with the symmetric mass split 126/126, the intermediate path (I) associated with the asymmetric mass split ~134/118, and the very asymmetric path (II) associated with the mass split ~146/106. The paths (I) and (II) go through the local HD minimum, $\rm HD_I$, at $\beta_2 \sim 1.0$ and $\beta_3 \sim 0.4$ and bypass a well-developed reflection-asymmetric third minimum, $\rm HD_{II}$, at $\beta_2 \sim 0.9$ and $\beta_3 \sim 0.65$. The potential energy curve corresponding to path (II) is shown in Fig. 4(b). The open dots in Fig. 4(a) and the dashed line in Fig. 4(b) indicate the static fission path from the minimum $\rm HD_{II}$. The density distribution in the HD minimum resembles a dinucleus. In the nuclear shape seen beyond point *B*, at $\beta_2 = 1.4$, in Fig. 4(b), the very elongated fragment *R* is predicted to be ^{146}Ba, in agreement with our experimental

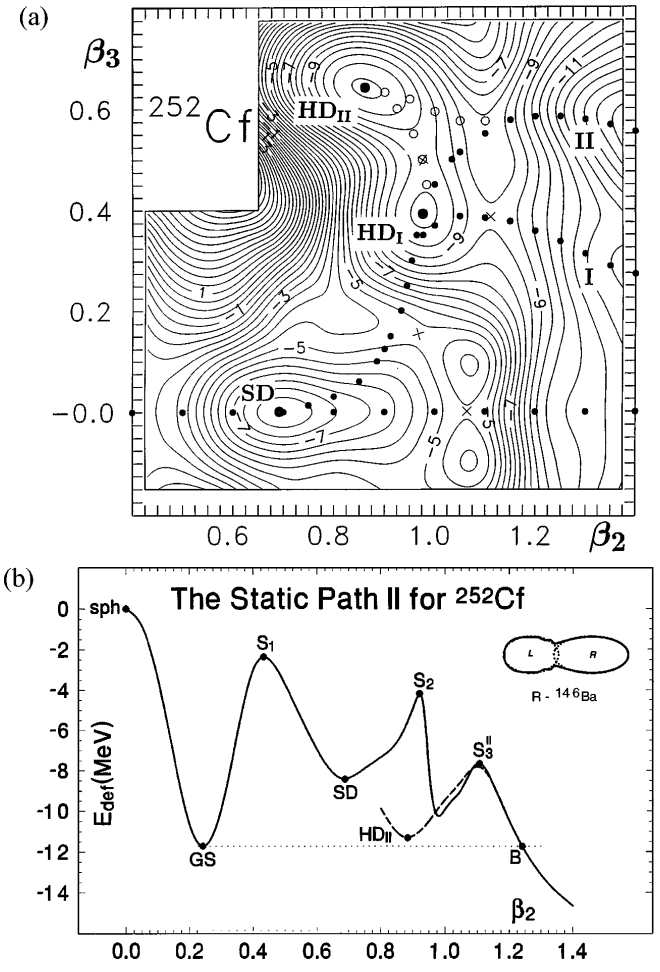

FIG. 4. (a) Potential energy surface for ^{252}Cf (relative to the energy at the spherical shape) as a function of β_2 and β_3. The minima (saddle points) are marked by filled dots (crosses). The dotted trajectories indicate three static fission paths: the reflection-asymmetric paths (I) and (II) and the symmetric path at $\beta_3 = 0$. (b) Potential energy curve for ^{252}Cf as a function of β_2 along the static fission path (II). The calculated shapes of ^{252}Cf in the minimum HD$_{II}$ ($\beta_2 \sim 0.9$, $\beta_3 \sim 0.65$) and at $\beta_2 = 1.4$ are shown together with the corresponding shapes of the left (L) and right (R) fragments.

results. However, it is difficult to say whether the observed HD fragments ^{144,145,146}Ba at scission can be associated with the direct decay of the third minimum or whether they bypass it. It would be fascinating to observe directly the HD$_{II}$ minimum in ^{252}Cf.

In conclusion, the observed coexistence of two fission modes in the spontaneous fission of ^{252}Cf involves a new type of bimodal fission. The striking feature of this new type bimodal fission with normal and low $\overline{\text{TKE}}$ is the manifestation of two distinct fission modes for the same charge/mass asymmetry for the Mo-Ba division of ^{252}Cf. So ^{144}Ba, ^{145}Ba, and/or ^{146}Ba are found in two states which are remarkable for their very different deformations at the scission, while their partners, ^{107,106}Mo, have approximately the same deformation in Modes 1 and 2 and ^{108}Mo a deformation near that of ^{144}Ba in Mode 2. The normal fission Mode 1 has features typical of the bulk of fission events of ^{252}Cf, while the abnormal Mode 2 reported here for the first time provides evidence for a HD shape for one or more of ^{144,145,146}Ba at scission.

G. M., T.-A., and A. V. D. express appreciation for the hospitality and financial support received from Vanderbilt. This work is supported in part by the U.S. DOE: DE-FG05-88ER40407 (Vanderbilt), DE-AC07-76ID01570(INEL), DE-FG05-93ER40770 (Tennessee); at JINR by Grant No. 94-02-05584-a of the Russian Federal Foundation of Basic Sciences; at the SAS Institute of Physics by the SAS Grant Agency Grant No. GA-SAV517/1993; the NSF Pittsburgh-Warsaw Grant No. INT-9115309, and by the Polish Committee for Scientific Research Contract No. 2 P03B 034 08. Oak Ridge National Laboratory is managed by Martin Marietta Energy Systems, Inc., under Contract No. DE-AC05-84OR21400 for the U.S. Department of Energy.

*Also at UNISOR, ORISE, Oak Ridge, TN 37832. On leave from the Institute of Nuclear Physics, Cracow, Poland.
†Current address: INEL, Idaho Falls, ID 83415.
‡Current address: Tsinghua University, Beijing, Peoples Republic of China.
§Current address: Lawrence Berkeley Laboratory, Berkeley, CA 94720.

[1] G. M. Ter-Akopian *et al.*, Phys. Rev. Lett. **73**, 1477 (1994).
[2] J. Wild *et al.*, Phys. Rev. C **41**, 640 (1990).
[3] M. G. Itkis *et al.*, Z. Phys. A **320**, 433 (1985).
[4] E. K. Hulet *et al.*, Phys. Rev. Lett. **56**, 313 (1986).
[5] V. Pashkevich, Nucl. Phys. **A169**, 275 (1971).
[6] P. Möller *et al.*, Nucl. Phys. **A469**, 1 (1987).
[7] S. Ćwiok *et al.*, Nucl. Phys. **A491**, 281 (1989).
[8] U. Brosa *et al.*, Phys. Rep. **197**, 167 (1990).
[9] J. H. Hamilton *et al.*, Prog. Part. Nucl. Phys. **35**, 635 (1995).
[10] J. H. Hamilton *et al.*, in Proceedings of the Workshop on Gammasphere Physics, edited by M. Delaplanque-Stephens (World Scientific, Singapore, to be published).
[11] A. C. Wahl, Nucl. Data Tables **39**, 1 (1988).
[12] P. G. Young *et al.*, in *Proceedings of the Workshop on Computation and Analysis of Nuclear Data Relevant to Nuclear Energy and Safety, Trieste, Italy, 1992* (World Scientific, Singapore, 1993).
[13] C. Budtz-Jørgensen and H.-H. Kittner, Nucl. Phys. **A490**, 307 (1988).
[14] S. Ćwiok *et al.*, Phys. Lett. B **322**, 304 (1994).